The temperature dependence of the polarizability of the free carriers in Germanium and Silicon

Autor(en): **Cardona, Manuel / Paul William / Brooks, Harvey**

Objekttyp: **Article**

Zeitschrift: **Helvetica Physica Acta**

Band (Jahr): **33 (1960)**

Heft V

PDF erstellt am: **21.09.2024**

Persistenter Link: https://doi.org/10.5169/seals-113078

The Temperature Dependence of the Polarizability of the Free Carriers in Germanium and Silicon*

by **Manuel Cardona****), **William Paul** and **Harvey Brooks**
Harvard University
Division of Engineering and Applied Physics, Cambridge, Massachusetts

(11. I. 1960)

Abstract. The reflectivity of n- and p-type Ge and Si at doping levels above 10^{18} carriers/cc has been measured at 297° K and 90° K at wavelengths from 2 to 20 microns. The contribution of the free carriers to the total electric polarizability was determined from the reflectivity, and hence an average effective mass for the carriers was deduced. An increase in electron mass with both carrier concentration and temperature was found in both n-type Ge and n-type Si. If both effects are assumed to originate from the non-parabolic character of the conduction band, then the effect of carrier concentration is too large compared with the effect of temperature, and both effects are too large to be compatible with estimates of the band gap at the zone boundary. No definite conclusions can be drawn about p-type Ge owing to transitions between branches of the degenerate valence band. For p-type Si the effective mass increases with temperature.

Introduction

The free carrier polarizability χ_c in a semiconductor is given in general by

$$\chi_c = \frac{e^2}{\hbar} \int \frac{\tau^2 v_x}{1+\omega^2\tau^2} \frac{\partial f_0}{\partial k_x} \frac{2}{(2\pi)^3} d\Omega_k \tag{1}$$

where e is the charge of the electron, $\hbar$ Planck's constant, τ the scattering time, v_x the group velocity of the carrier in the field direction, ω the angular frequency, f_0 the Fermi distribution function, k_x the component of crystal momentum in the field direction, and $d\Omega_k$ the element of volume in k-space. For Ge and Si in the infrared region we may write $\omega\tau \gg 1$ and equation (1) may be written:

$$\chi_c = \frac{1}{4\pi^3} \frac{e^2}{\omega^2} \int v_x^2 \frac{\partial f_0}{\partial E} \frac{dS_k}{|\nabla_k E|} dE \tag{2}$$

* This work was supported by the United States Office of Naval Research under Contract Nonr 1866 (10).

** Now of Laboratories R. C. A. Ltd., Zurich, Switzerland.

where dS_k is an element of a surface of constant energy E. For parabolic bands, and ellipsoidal energy surfaces equation (2) may be integrated to give the familiar result

$$-\chi_c = \frac{Ne^2}{m^*\omega^2} \tag{3}$$

where N is the carrier density and m^* is the average effective mass given by

$$\frac{3}{m^*} = \frac{1}{m_{\parallel}} + \frac{2}{m_{\perp}} \tag{4}$$

where $m_{\parallel}$ and $m_{\perp}$ are the longitudinal and transverse effective masses, respectively*.

For p type Ge, assuming concentric spherical energy surfaces and parabolic bands we would have

$$\frac{1}{m^*} = \frac{m_{lh}^{1/2} + m_{hh}^{1/2}}{m_{lh}^{3/2} + m_{hh}^{3/2}} \tag{4'}$$

where m_{lh} and m_{hh} refer to the light and heavy holes, respectively. If equation (4) were valid the effective mass deduced from (4') would be about 3/4 the heavy hole mass, or about 0·3 electron masses. In practice (4') is not valid because of non-parabolic effects, and furthermore (1) and (2) fail because of interband transitions. If the temperature is low enough so that the number of carriers in the lower band split by spin-orbit interaction is small, equation (4') is also applicable to p-type silicon.

Method

(1) Reflectivity Measurements.

The polarizability was determined from reflectivity measurements. The reflectivity for normal incidence is given by

$$R = \frac{(n-1)^2+\nu^2}{(n+1)^2+\nu^2} \tag{5}$$

where n is the refractive index and ν the extinction index which can be

* In deriving equation (1) the internal electric field is assumed equal to the external applied field, i. e. the Lorentz correction is assumed to vanish. For a justification of this fact in the present case see D. PINES and P. NOZIERES, Phys. Rev. *109*, 762 (1958). Also strictly speaking, the approximation in going from (1) to (2) requires close examination, since the impurity scattering time becomes very small for low carrier energy. A rough analysis shows that the condition for the validity of (2) is that $E_c \ll 2 \cdot 4kT$, where E_c is the carrier energy for which $\omega\tau \approx 1$. Since the correction term varies with frequency as $\omega^{-11/3}$ the fact that no deviation from an ω^{-2} frequency dependence is observed constitutes additional evidence for the validity of (2).

determined from transmission measurements. The polarizability is then found from:

$$\varepsilon = \varepsilon_0 + 4\pi\chi_c = n^2 - \nu^2 \tag{6}$$

where ε is the dielectric constant and ε_0 the (intrinsic) dielectric constant with no free carriers present.

The reflectivity of the samples was measured by comparison with an intrinsic germanium sample. The reflectivity of intrinsic germanium at wavelengths longer than those corresponding to the absorption edge (1·5 μ) can be calculated by setting $\nu = 0$ in equation 5 and using the values of the intrinsic refractive index and its temperature coefficient reported by the authors[2]). At wavelengths longer than 5 microns, the reflectivity of intrinsic germanium is wavelength independent within our experimental accuracy ($\sim 1\%$).

The samples to be measured were cut in slabs of 1 mm thickness and about 1 cm² in area. One side of the slabs was optically polished with Linde A-5175 (rough polish)*) and Gamal (final polish)**). Whenever a sample was polished several times, the reflectivity was found to be reproducible within an error of 5% which can be attributed to sample alignment. The samples were mounted inside a cryostat with a single KBr window to let the radiation in and out. An angle of incidence of 5° was used to separate the incoming from the outgoing beam. Under these conditions, it can be shown that the departure from equation (5) is only of the order of 0·1%.

A Perkin-Elmer 12C spectrometer with KBr optics was used. The source of radiation was a globar and the detector a Reeder***) radiation thermocouple.

2. Hall Measurements

(2) *Hall Measurements.*

At the high carrier concentrations used in these measurements, the impurity levels are merged with the conduction or valence band, hence, the number of carriers N is temperature independent. A knowledge of the number of carriers is not required to determine the percentage change of the effective mass with temperature, but is necessary to obtain the magnitude of the effective mass. An estimate of the number of carriers can be made from Hall effect measurements. At temperature such that $kT \ll E_F$ (E_F is the Fermi level measured from the band edge) the Hall coefficient for n type germanium or silicon is given by:

$$R_H = \frac{3}{\mathrm{Nec}} \frac{K_H (K_H+2)}{(1+2K_H)^2} \tag{7}$$

* Linde Air Products Company, New York, New York.

** Fisher Scientific Company, Fairtown, New York.

*** Charles M. Reeder and Company, Detroit 3, Michigan.

where $$K_H = \frac{K_m}{K_\tau}, \quad K_m = \frac{m_\parallel}{m_\perp} \text{ and } K_\tau = \frac{\tau_\parallel}{\tau_\perp}.$$

$\tau_\parallel$ is the longitudinal component of the scattering time tensor and $\tau_\perp$ the transverse component. If the scattering time is isotropic ($K_\tau = 1$) we obtain:

$$\frac{3\,K_H\,(K_H+2)}{(2\,K_H+1)^2} = 0{\cdot}79 \text{ for germanium}$$

$$\frac{3\,K_H\,(K_H+2)}{(2\,K_H+1)^2} = 0{\cdot}87 \text{ for silicon}$$

The scattering by ionized impurities, which is the dominant scattering mechanism in our samples, is strongly anisotropic[4]). The anisotropy of τ decreases the value of K_H. Values of K_H as low as 4 have been found in impure germanium from magnetoresistance measurements[6]). Ham[5]) calculated K_τ for pure ionized impurity scattering using an extension of the Brooks-Herring treatment and found $K_\tau = 12$ for germanium and $K_\tau = 4$ for silicon. The values of $3\,K_H(K_H+2)/(2\,K_H+1)^2$ found from this analysis differ from 1 by less than 5%. However, Ham's analysis is not valid for the high carrier concentrations existing in our samples. The large anisotropy in his calculations arises from the predominance of forward scattering when the ionized impurities are only slightly screened. In heavily doped samples, in which the impurities are strongly screened, the scattering is more nearly isotropic, and hence the scattering time depends much less strongly on the initial direction of the electron, with the result that K_τ probably does not exceed 2 in our samples.

Despite this, because of the absence of experimental determinations for samples of this doping, we have taken the factor $3\,K_H(K_H+2)/(2\,K_H+1)^2$ as equal to unity. Any error in this assumption will affect only the absolute magnitude of the deduced effective mass and not its percentage change with temperature.

For p-type germanium and silicon, the situation is complicated by the degeneracy of the valence band at $k = 0$. If for germanium we assume spherical energy surfaces, isotropic scattering, and neglect the split-off band, then with degenerate statistics we obtain:

$$R_H = \frac{1}{\text{Nec}} \frac{\left(m_l^{-1/2}\,\tau_l^2 + m_h^{-1/2}\,\tau_h^2\right)\left(m_l^{3/2} + m_h^{3/2}\right)}{\left(m_l^{1/2}\,\tau_l + m_h^{1/2}\,\tau_h\right)^2} \tag{8}$$

where τ_l and τ_h are the scattering times for the holes in the light and heavy mass bands, respectively. Unfortunately, very little can be said regarding the ratio of τ_l/τ_h for the high impurity concentrations used in these measurements. For these concentrations possibly the most plausible assumption is $\tau_l = \tau_h$, which substituted in equation (8) would lead to $R_H \cong 2/\text{Nec}$. Some microchemical evidence[17]) suggests that $R_H \approx 1/\text{Nec}$.

In the absence of definite information we have taken $R_H = 1/\mathrm{Nec}$, although this assumption is even less reliable than in the case of n-type germanium.

Results

(1) *n-type germanium.* The reflectivity of nine n-type germanium samples was measured at 297° K and 90° K (see Table 1). Their carrier

Table 1
Heavily Doped Samples and Results of Reflectivity Measurements

Material	Origin	Source Identification Mark	Carriers/cm³	$\frac{m^*(297°\,\mathrm{K}) - m^*(90°\,\mathrm{K})}{m^*(297°\,\mathrm{K})} \times 100$	$\frac{m^*}{m}$
Ge, n-type	R. C. A.	1787	$5{\cdot}2\times 10^{19}$	6	0·26
Ge, n-type	Westinghouse	12	$4{\cdot}4\times 10^{19}$	6	0·24
Ge, n-type	Bell	1136	$1{\cdot}1\times 10^{19}$	5	0·21
Ge, n-type	Raytheon	322	$3{\cdot}7\times 10^{18}$	9	0·14
Ge, n-type	Raytheon	Pa	$2{\cdot}0\times 10^{18}$	7	0·14
Ge, n-type	Westinghouse	PK	?	10	?
Ge, n-type	Westinghouse	5	?	8	?
Ge, n-type	Lincoln	985	?	6	?
Ge, n-type	G. E.	112	?	9	
Ge, p-type	R. C. A.	1781	6×10^{19}		
Ge, p-type	I. B. M.	44	$2{\cdot}5\times 10^{19}$		
Ge, p-type	Lincoln	1017	$2{\cdot}4\times 10^{19}$		
Ge, p-type	Westinghouse	59	8×10^{18}		
Si, n-type	Bell	445	$1{\cdot}1\times 10^{20}$	10	0·44
Si, n-type	Bell	427 I	$6{\cdot}5\times 10^{19}$	9	0·44
Si, n-type	Bell	427 II	$6{\cdot}4\times 10^{19}$	9	0·43
Si, n-type	Bell	427 III	$6{\cdot}4\times 10^{19}$	9	0·43
Si, p-type	Sylvania	Sy	?	12	?

concentrations were determined from Hall measurements as discussed in the previous section. Several samples were cut from the same reflectivity specimen and the uniformity of the carrier concentration was checked. A question mark in the N column of Table 1 indicates samples whose carrier concentration was not uniform. These samples were not suitable for absolute effective mass measurements, but they were used for temperature coefficient determinations. The estimated accuracy in the effective mass measurements was 10%, corresponding to the error in the determination of the Hall constant. Figures 1 and 2 show the reflectivity of 4 n-type germanium samples at 90° K and 297° K. For small wave-

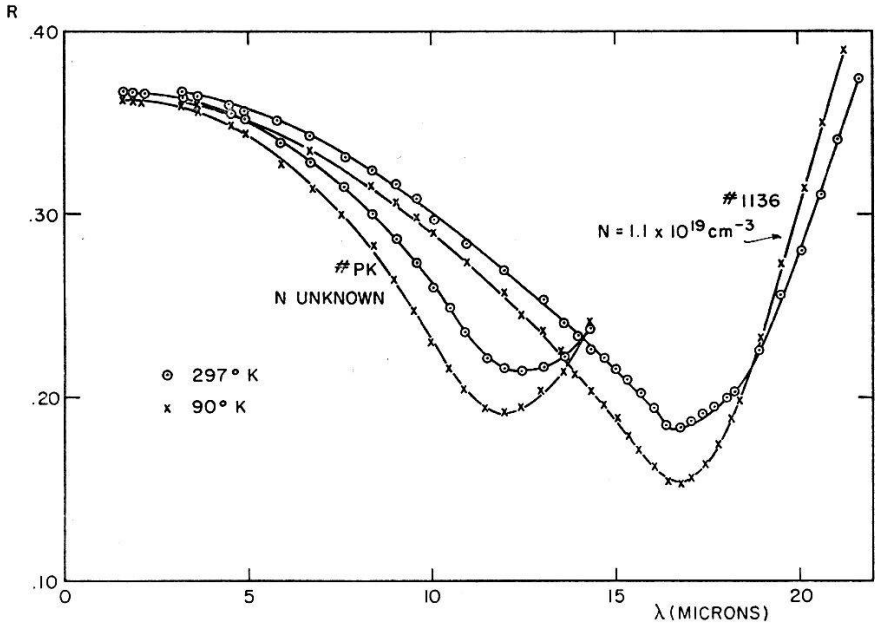

Fig. 1
Wavelength dependence of the reflectivity of heavily doped *n*-type germanium

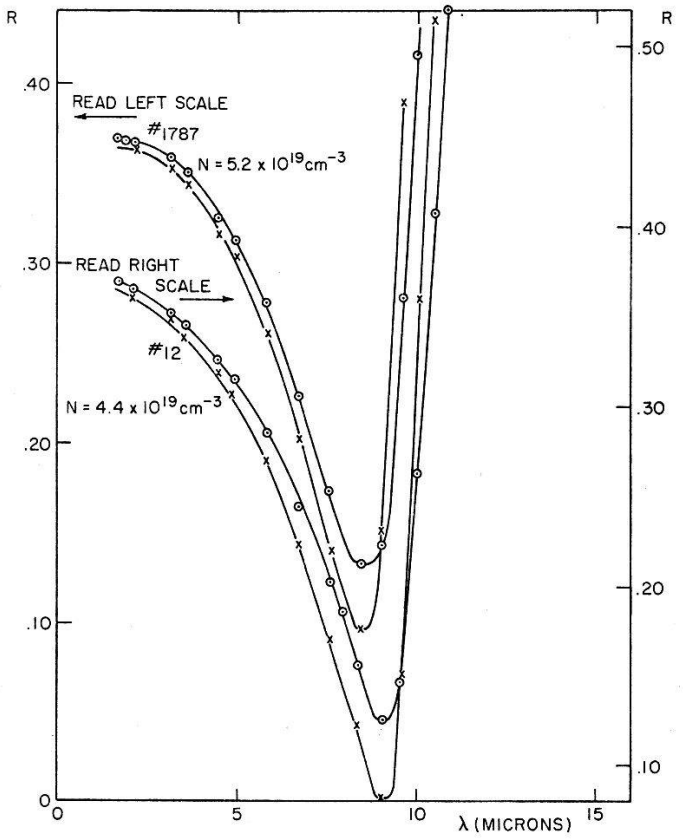

Fig. 2
Wavelength dependence of the reflectivity of heavily doped *n*-type germanium

lengths, the reflectivity decreases with increasing wavelength due to the decreasing refractive index. At a certain wavelength, the reflectivity goes through a minimum and starts to increase sharply due to the sharp increase of the extinction index. Since ν depends on carrier mobility as well as effective mass, the rising portions of these curves were not used to obtain information about the mass. At wavelengths much shorter than the minimum, ν can be neglected in equation (5). Close to the minimum ν has to be measured to determine n from the reflectivity. Figure 3 shows

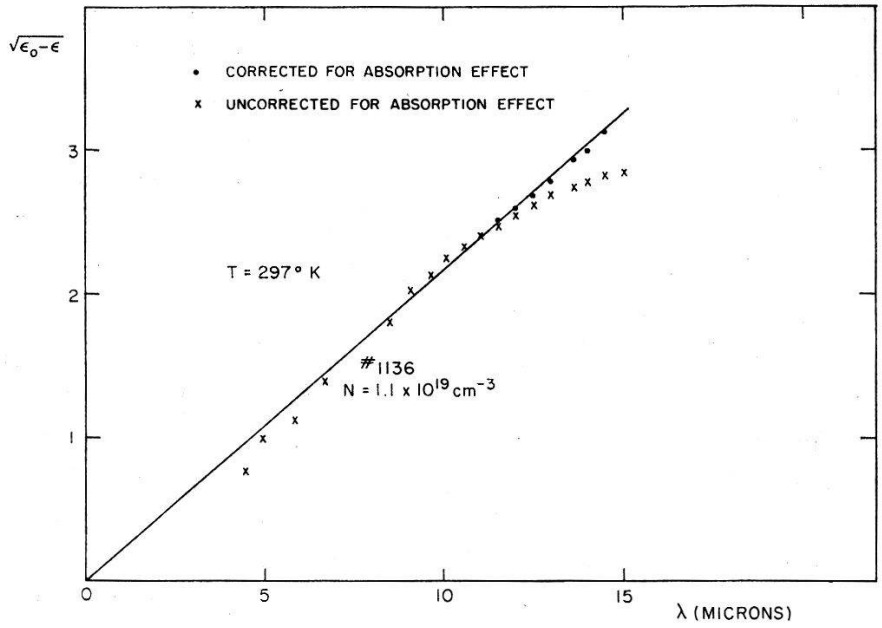

Fig. 3
Square root of the free carrier contribution to the dielectric constant in n-type germanium

$\sqrt{\varepsilon_0 - \varepsilon}$ as a function of wavelength calculated from the reflectivity first by assuming $\nu = 0$ and second by using the measured value of ν. The results differ only close to the reflectivity minimum because ν increases very rapidly with increasing wavelength. The measurement of ν is not necessary if we determine m^* solely from the linear portion of the curve of $\sqrt{\varepsilon_0 - \varepsilon}$ against λ, for $\nu = 0$.

Table 1 indicates the values of the effective masses obtained by this technique. An increase in effective mass with increasing carrier concentration was observed. While these values are subject to the error of assuming $K_H = 1$ in the Hall formula, it is unlikely that variations in K_H can account for the observed effective mass variation with carrier concentration.

The effective mass obtained for the lowest carrier concentrations measured ($m^* = 0{\cdot}14$ m) is the same as the value found by Spitzer and Fan for similar carrier concentrations (4×10^{18} cm^{-3}). This value is also in fair agreement with the value calculated from the cyclotron resonance

effective masses ($m^* = 0{\cdot}12$ m), especially since the error in the Hall effect formula is such as to overestimate the effective mass ($R_H = 0{\cdot}85/nec$ corresponds to $m^* = 0{\cdot}12$ m). Specific heat measurements on a heavily doped germanium sample of similar carrier concentration ($N = 4{\cdot}7 \times 10^{18}$ cm^{-3}) also gave an effective mass in agreement with the corresponding value of the cyclotron resonance effective mass[7]). An effective mass for heavily doped n-type germanium was determined by BOWERS[8]) and by STEVENS *et al.*[9]) from diamagnetic susceptibility measurements*). The diamagnetic susceptibility of the free carriers is, for degenerate samples, proportional to $N^{1/3}$, hence, accurate determinations of N are not as important as in our experiments for the determination of the effective mass. Unfortunately, the results obtained by these authors are not in agreement. While STEVENS *et al.* found an increase in effective mass with carrier concentration in qualitative agreement with our results, a constant effective mass for carrier concentrations as high as 3×10^{19} cm^{-3} was reported by BOWERS. No estimate of the accuracy of their measurements was given by these authors.

An average increase of ($7 \pm 3\%$) in the effective mass of n-type germanium was found between 90° K and 297° K. No dependence of this increase on the carrier concentration could be observed within our experimental accuracy (see Table 1). GEIST[10]) estimated the effective mass in n-type germanium ($N = 8 \times 10^{16}$ cm^{-3}) from magnetic susceptibility measurements. He found $m^* = 0{\cdot}16$ m at 138° K and $m^* = 0{\cdot}19$ m at 297° K. The accuracy of this determination is not known, but the agreement with our measurements seems reasonable.

MCFARLANE *et al.*[11]) determined the temperature variation of the combined average of the electron and hole effective masses which appears in the expression

$$N_i = 4{\cdot}8 \times 10^{15} \left(\frac{\overline{m}}{m}\right)^{-3/2} N_m^{1/2}\, T^{3/2} \exp\,(-E_g/2\,kT) \qquad (9)$$

where $N_m = 4$ in germanium, E_g is the thermal energy gap and:

$$\overline{m} = (m_\perp^2\, m_{\|}\, m_h^3)^{1/6}$$

(m_h is the appropriate average of the heavy and light hole effective masses). For a temperature increase of 200° C MCFARLANE *et al.* found an increase of about 10% in $\overline{m}$. Direct comparison between these results

* The effective mass average found from diamagnetic susceptibility measurements is not the same average as found from electric polarizability measurements. The magnetic susceptibility effective mass calculated from the cyclotron resonance masses is $m^* = 0{\cdot}14$ m in n-type germanium while the reflectivity effective mass is $m^* = 0{\cdot}12$ m. As these values are very close and mainly determined by the transverse effective mass, their temperature behaviour should be similar.

and ours is not possible as $\bar{m}$ involves the hole effective masses. If the temperature coefficient of the hole effective masses were close to that of the electron effective masses, the results of McFARLANE *et al.* would be in agreement with ours.

According to Herring*) the deviation in the temperature dependence of the mobility of n-type germanium ($\alpha\ T^{-1.66}$) from the theoretical acoustical scattering law ($\alpha\ T^{-1.50}$) must be due to temperature dependence of the effective mass or the deformation potential constant. If the latter is assumed constant, as the mobility is proportional to $m^{*-5/2}$, a temperature increase in m^*/m of 8% between 90 and 270° K would be necessary to account for the quoted discrepancy of the mobility law. This effective mass variation is in good agreement with our result.

2. *n-type silicon.* The reflectivity of four n-type silicon samples was measured at 297° and 90° K (see Table 1). Figure 4 shows the spectral

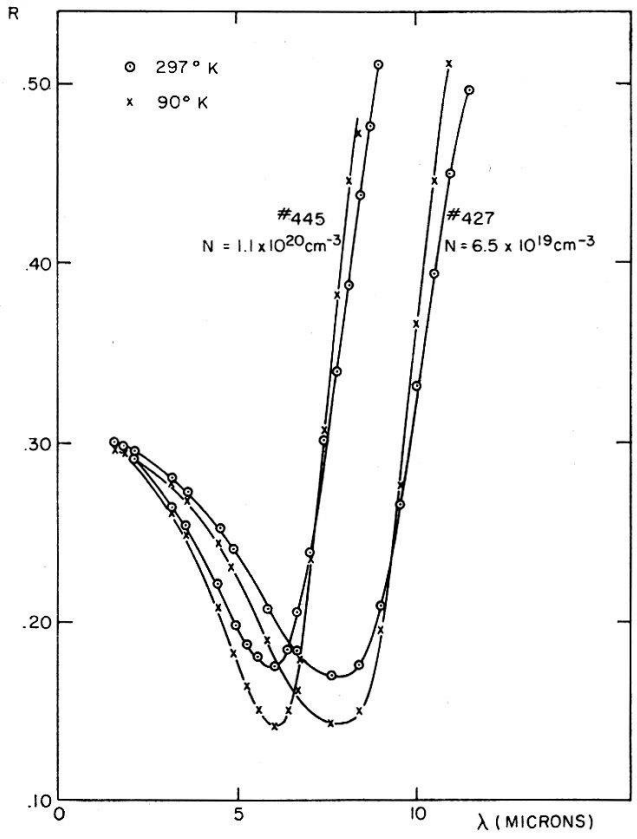

Fig. 4
Wavelength dependence of the reflectivity of heavily doped n-type silicon

and temperature dependence of the reflectivity of two n-type silicon samples. The shape of the curves in figure 4 is similar to the shape of the corresponding curves for n-type germanium. The effective masses ob-

* C. HERRING, American Physical Society Meeting, Cambridge, Massachusetts, March 1959. Unpublished.

tained ($m^* = 0{\cdot}44$ m) were higher than the value found by SPITZER and FAN ($m^* = 0{\cdot}27$ m) for a sample of lower carrier concentration ($N = 3{\cdot}6 \times 10^{18}$ cm^{-3}). This discrepancy indicates a possible increase of m^* with increasing number of carriers as in the case of germanium. On the other hand doubling the carrier concentration from sample 427I to 445 in our measurements gave no significant change in effective mass. KEESOM and SEIDEL[7]) found for $N = 10^{19}$ cm^{-3} $(m_\perp^2\, m_\parallel)^{1/3} = 0{\cdot}42$ m, while the value found from the cyclotron resonance effective masses is 0·33 m. The discrepancy between these two values is in qualitative agreement with the postulated increase in effective mass with increasing carrier concentration.

SONDER and STEVENS[12]) determined the effective mass of heavily doped n-type silicon from the diamagnetic susceptibility of the free carriers. For a carrier concentration $N = 5 \times 10^{18}$ cm^{-3}, they found an average effective mass $m^* = 0{\cdot}29$ m, in good agreement with the average determined from the cyclotron resonance effective masses ($m^* = 0{\cdot}28$ m). At higher carrier concentration ($2{\cdot}9 \times 10^{19}$ cm^{-3}) they found a larger effective mass ($m^* = 0{\cdot}38$ m) in fair agreement with our conclusions.

An average increase of ($10 \pm 3\%$) in the effective mass of n-type silicon was observed between 90 and 297° K (see Table 1). An increase of 10% was also found by SONDER and STEVENS[12]) and GEIST[10]) in the same temperature range from magnetic susceptibility measurements. MCFARLANE *et al.*[13]) found an increase in the average electron-hole effective mass of equation 9 of about 20% for a temperature increase of 200° K. The error of this determination was at least 50% of the increase found. If the temperature behaviour of the hole effective mass is roughly the same as that of the electron effective mass (see next section), qualitative agreement between these results and ours would be found.

3. *p-type silicon.* Figure 5 shows the reflectivity of a p-type silicon sample as a function of wavelength and temperature. The behavior of this curve is similar to that for n-type germanium and silicon. The interband transitions between the various branches of the valence band do not affect the reflectivity in the region of measurement of figure 5, as they occur at much longer wavelengths (about 30 microns). The free carrier effective mass was not determined, as the carrier concentration was not uniform in the only sample available. An increase with temperature of 12% for the average effective mass was found between 90 and 297° K. Due to the small spin orbit splitting in the valence band, the average of the effective masses at room temperature includes not only the light and heavy hole masses, but also some contribution of the hole mass in the third band lowered in energy by the spin orbit splitting. The average heavy and light hole effective masses are $m_{hh} = 0{\cdot}50$ m and

$m_{lh} = 0{\cdot}17$ m for silicon, and the optical effective mass of equation (4′) is $m^* = {\cdot}38$ m. The heavy hole band is parabolic in KANE's[22]) approximation but the light hole band flattens out as the energy increases until it becomes parallel to the heavy hole band. Hence, an increase in the

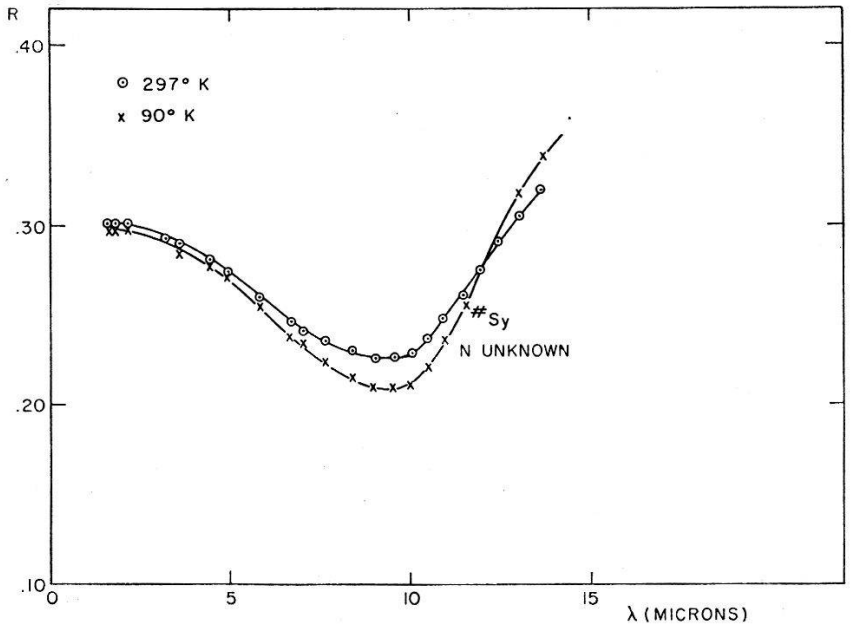

Fig. 5
Wavelength dependence of the reflectivity of heavily doped p-type silicon

effective mass with increasing temperature is to be expected due to the higher population of the higher effective mass states in the light mass valence band. No attempt at a quantitative estimate of this effect has been made.

4. *p-type germanium.* Figure 6 shows the reflectivity of two p-type germanium samples as a function of wavelength and temperature. The behavior of the reflectivity of p-type germanium differs from that of the preceding materials. This difference is due to the presence of transitions between the various valence band branches in the spectral region of the measurement[14]). The absorption coefficient K due to these interband transitions can be found from the matrix elements for the transitions and the energy bands calculated by KANE[22]). The expression for the absorption coefficient for the vertical transition between energy E_1 and energy E_2 at wave vector k is:

$$K = \frac{2\,e^2\,k^3\,W_{12}\left\{f_0\left(\frac{E_1-E_F}{kT}\right) - f_0\left(\frac{E_1-E_F}{kT}\right)\right\}}{n\hbar c\,(E_1-E_2)\left(\frac{dE_1}{dk^2} - \frac{dE_2}{dk^2}\right)} \qquad (9')$$

where W_{12} is the quantity defined by KANE (eq. 36, p. 92 of ref. 22), and is related to the square of the matrix element for the transition. Inspec-

tion of KANE's Fig. 6 (p. 93 of ref. 22) and Fig. 2 (p. 88) indicates that, for the (110) direction at least, W_{12} is quite accurately proportional to $[dE_1/dk^2 - dE_2/dk^2]$. Using this result, together with the constant of proportionality estimated from Kane's curves, we have computed K for

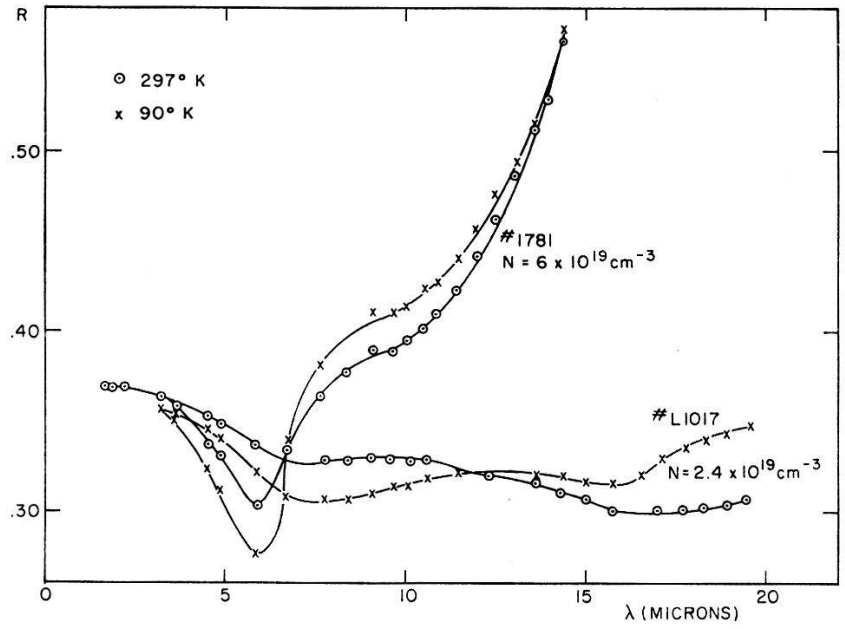

Fig. 6
Wavelength dependence of the reflectivity of heavily doped p-type germanium

the transitions between the two hole bands degenerate at $k = 0$ at 90° K and 297° K for a hole concentration of $2{\cdot}2 \times 10^{19}$ cm^{-3}. Figure 7 shows the result obtained as a function of wavelength. The cut-off at $7{\cdot}2\,\mu$ corresponds to the bands becoming parallel as k increases. The maximum in the absorption coefficient at $7{\cdot}2\,\mu$ probably explains the hump at about $9\,\mu$ in the reflectivity curves of Figure 6.

The polarizability corresponding to these transitions can be found from:

$$\varepsilon - \varepsilon_0 = \frac{2c}{\pi} \int \frac{n_1 K(\omega_1) d\omega_1}{\omega_1^2 - \omega^2} \qquad (9'')$$

We have estimated $\varepsilon - \varepsilon_0$ by substituting in (9″) $n_1 \approx \sqrt{\varepsilon_0}$ as found at $\lambda = 6\,\mu$:

$$\left.\begin{aligned} \varepsilon - \varepsilon_0 &= -\,4{\cdot}3 \text{ at } 297^0 \text{ K} \\ \varepsilon - \varepsilon_0 &= -\,5{\cdot}6 \text{ at } 90^0 \text{ K} \end{aligned}\right\} \text{ A}$$

This result qualitatively accounts for the minimum reflectivity found at $\lambda = 7\,\mu$ and its temperature dependence. At $\lambda = 6\,\mu$ we find from Figure 6:

$$\left.\begin{aligned} \varepsilon - \varepsilon_0 &= -\,2{\cdot}3 \text{ at } 297^0 \text{ K} \\ \varepsilon - \varepsilon_0 &= -\,3{\cdot}3 \text{ at } 90^0 \text{ K} \end{aligned}\right\} \text{ B}$$

Hence, we must conclude that there is a positive polarizability due to transitions between the lower split off band and the upper valence bands which compensates the negative free carrier polarizability and accounts

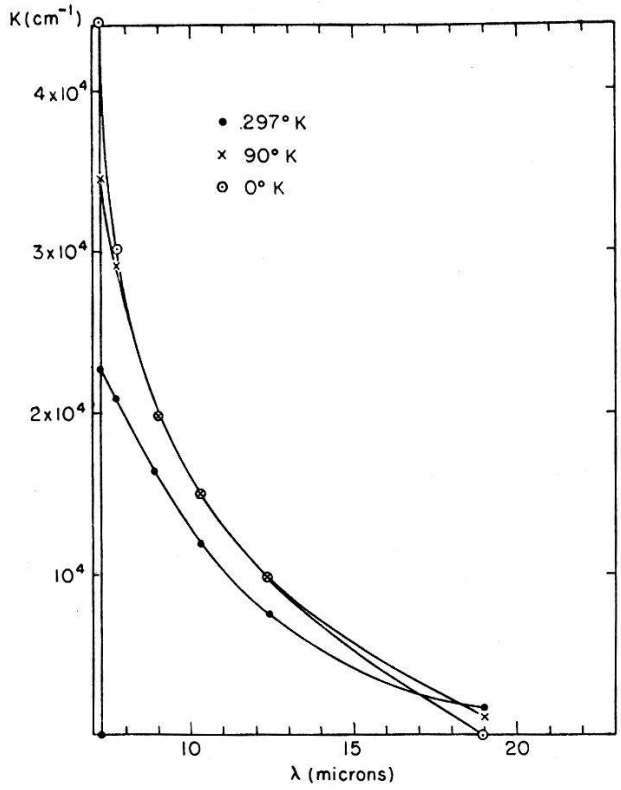

Fig. 7
Calculated absorption coefficient for p-type germanium with $2{\cdot}2\times 10^{19}$ carriers $\times$ cm^{-3} due to interband transitions

for the difference between A and B. Under these circumstances, no reliable values of the effective mass can be obtained from reflectivity measurements.

5. *Discussion.* The temperature variation of the effective mass can be divided into two contributions, one due to the thermal expansion of the lattice and the other an explicit effect of temperature. The effect of the thermal expansion can be estimated from the pressure dependence of the effective mass. NATHAN[15]) estimated for n-type germanium an increase in the average effective mass of $(5 \pm 5)\%$ in 10000 kg/cm^2. Hence, if the variation of the effective mass with temperature were due to the volume effect only, a decrease of $(2 \pm 2)\%$ between 90° K and 297° K would be expected, whereas an increase was actually found. This shows that the explicit temperature effect is larger than the volume effect and has the opposite sign. The explicit temperature effect can be divided into two contributions, one due to a change in the curvature at the band extremum and the other the result of the spread with temperature of the Fermi distribution in a non parabolic band.

In order to estimate this last effect we assume for the energy in the neighborhood of the (111) minimum of the conduction band an expression of the form:

$$E = -\Delta + \alpha k_z^2 + \sqrt{\Delta^2 + \beta^2 (k_x^2 + k_y^2)} \tag{10}$$

where 2Δ is the energy separation between the (111) minimum of the conduction band (L_1) and the L_3' energy of the valence band. An expression of this form would correspond to the interpretation given by PHILLIPS[18]) for the relative intensity of the absorption edge at 2·1 ev. reported by PHILLIP and TAFT[19]. However, there is some ambiguity in this result, which will not seriously affect our conclusions. The constants α and β are related to the longitudinal and transverse masses at the bottom of the band by:

$$\frac{1}{m_\perp} = \frac{\beta^2}{\Delta\hbar^2} \qquad \frac{1}{m_\parallel} = \frac{2\alpha}{\hbar^2}$$

By substituting equation (10) into equation (2) the following approximate expression for the effective mass in equation (3) is found (see Appendix A):

$$\frac{3}{m^*} = \left(\frac{1}{m_\parallel} + \frac{2}{m_\perp}\right)\left[1 - \frac{4}{3\left(1+\frac{m_\perp}{2m_\parallel}\right)\Delta}\,\frac{\int_0^\infty f_0\, E^{3/2} dE}{\int_0^\infty f_0\, E^{1/2} dE}\right] \tag{11}$$

The Fermi level is given exactly for equation (10) by the solution of:

$$N = n_m \frac{\sqrt{2}\, m_\parallel^{1/2}\, m_\perp}{\pi^2\hbar^3} \int_0^\infty E^{1/2}\left(1 + \frac{2E}{3\Delta}\right) f_0\left(\frac{E - E_F}{kT}\right) dE \tag{12}$$

where n_m is the number of minima in the conduction band. For classical statistics, equation 11 becomes

$$\frac{3}{m^*} = \left(\frac{1}{m_\parallel} + \frac{2}{m_\perp}\right)\left[1 - \frac{2}{1+\frac{m_\perp}{2\, m_\parallel}}\,\frac{kT}{\Delta}\right] \tag{13}$$

More generally the result may be written

$$\frac{3}{m^*} = \left(\frac{1}{m_\parallel{}^*} + \frac{2}{m_\perp}\right)\left[1 - \frac{4\,kT}{3\left(1+\frac{m_\perp}{2m_\parallel}\right)\Delta}\,\frac{\int_0^\infty x^{3/2} f_0\,(x-\eta)dx}{\int_0^\infty x^{1/2} f_0\,(x-\eta)dx}\right] \tag{14}$$

Δ can be estimated from the expriments of PHILIPP and TAFT[19]), who find a strong increase in the absorption coefficient of germanium at about 2 *ev*. This absorption has been ascribed to the $L_1 - L_3'$ energy gap[18]).

ROTH and LAX[20]) estimated $\Delta = 0{\cdot}8$ ev. from the anisotropy of the g-factor of shallow donor levels in germanium at 4° K. They suggested that an increase in Δ with temperature might be responsible for the difference between this value of Δ and the one found by PHILIPP and TAFT, but this result is subject to further confirmation. In our calculations we have taken the average value $\Delta = 0{\cdot}9$ ev. With this assumption, equation (13) yields an increase of 3·9% in $1/m^*$ between 90° K and 297° K. The calculated values of the second term in brackets in eq. (14) are listed in Table 2 for several carrier concentrations. Table 2 shows that the increment of the effective mass between 297° K and 90° K decreases with increasing carrier concentration. Nevertheless, the value of $(m^*/m)_{297°\,K} - (m^*/m)_{90°\,K}$ for the sample of lowest carrier concentration measured only differs from the value for the highest carrier concentration by about 1·5% and this change cannot be detected within our large experimental error (3%).

The increase in effective mass shown in Table 2 is about half that observed. This must be due either to a smaller value of Δ than we have

Table 2
Theoretical Effective Mass for n-type Ge for Various Cases, where

$$\left(\frac{m}{m^*}\right)_{0°\,\mathrm{K.,\,class.}} = \frac{1}{3}\frac{m}{m_\parallel} + \frac{2}{3}\frac{m}{m_\perp}, \quad m_\parallel = 1{\cdot}58\,m \quad m_\perp = 0{\cdot}084\,m$$

	E_F(ev)			$\dfrac{\left(\frac{m^*}{m}\right)_{T°\,\mathrm{K}} - \left(\frac{m^*}{m}\right)_{0°\,\mathrm{K.,\,class.}}}{\left(\frac{m^*}{m}\right)_{0°\,\mathrm{K.,\,class.}}}$			$\dfrac{\left(\frac{m^*}{m}\right)_{297°\,\mathrm{K}} - \left(\frac{m^*}{m}\right)_{90°\,\mathrm{K}}}{\left(\frac{m^*}{m}\right)_{0°\,\mathrm{K.,\,class.}}}$
	0° K	90° K	297° K	0° K	90° K	297° K	
Classical Statistics				0	·0168	·0554	·0386
N = 5×10^{18} cm^{-3}	·019	·015	·016	·0158	·0248	·0580	·0332
N = 10^{19} cm^{-3}	·030	·029	·0064	·0256	·0319	·0642	·0323
N = 5×10^{19} cm^{-3}	·087	·085	·079	·0748	·0774	·0977	·0202

estimated or to a decrease in the band extremum curvature with increasing temperature. The latter would require only about a 3% change in band gap with temperature and does not seem unlikely. This does not correspond to the pressure results of NATHAN[15]), if one assumes that the change in band gap is wholly due to the change in lattice constant with temperature.

Table 2 also enables us to estimate the influence of doping on the apparent effective mass. This changes the reciprocal mass by a maximum of 10% from the value at low doping. However, we see from Table 1 that doping nearly halves the reciprocal mass for the highest carrier concentration. The discrepancy is in the same direction as for the temperature effect, but is considerably larger. It would require an unreasonably small value of Δ. It would seem more likely that there exists an explicit effect on the band curvature due to the high impurity content.

6. *Acknowledgements*. The present work would not have been possible without the cooperation of a great many individuals and industrial laboratories who supplied the samples used in the measurements. The samples listed in Table 1 were obtained through the kindness of Drs. M. C. STEELE from R. C. A., R. BOWERS from Westinghouse, J. PATEL from RAYTHEON, W. W. TYLER from G. E., M. I. NATHAN from I. B. M., W. G. SPITZER from Bell and P. MOODY from Lincoln Laboratory.

Appendix A

The condition for the determination of the FERMI level may be written:

$$N = \frac{1}{4\pi^3}\int f_0\left(\frac{E-E_F}{kT}\right) d\Omega_k = \frac{1}{4\pi^3}\int_0^\infty dE\, f_0\left(\frac{E-E_F}{kT}\right)\int_E \frac{dS_k}{|\nabla_k E|} \quad \text{(A.1)}$$

Similarly, by comparison of equation (2) and (3) we see that the effective mass tensor may be written:

$$\frac{N}{\boldsymbol{m}^*} = -\frac{1}{4\pi^3\hbar^2}\int_0^\infty dE\,\frac{\partial f_0\left(\frac{E-E_F}{kT}\right)}{\partial E}\int_E \nabla_k E \nabla_k E\,\frac{dS_k}{|\nabla_k E|} \quad \text{(A.2)}$$

where in (A. 1) and (A. 2) the second integral is taken over a surface of constant energy E.

If we assume that each surface of constant energy is a surface of revolution and take k_z along the revolution axis, then if $E = f(k_\rho, k_z)$ in cylindrical coordinates we find:

$$\frac{dS_k}{|\nabla_k E|} = \frac{1}{2}\frac{dk_\varrho^2}{dE}\,dk_z\,d\varphi \quad \text{(A.3)}$$

where φ is the angle about the axis of revolution. Since the overall symmetry of the energy surfaces is cubic, the tensor derivative in equation (A. 2) may be replaced by the scalar

$$\frac{1}{3}\nabla_k E \cdot \nabla_k E$$

so that (A. 2) becomes:

$$\frac{N}{m^*} = -\frac{1}{4\pi^2\hbar^2}\int_0^\infty dE\,\frac{\partial f_0\left(\frac{E-E_F}{kT}\right)}{\partial E}\int_E \frac{1}{3}\left[\left(\frac{\partial E}{\partial k_\varrho}\right)^2+\left(\frac{\partial E}{\partial k_z}\right)^2\right]\frac{dk_\varrho^2}{dE}\,dk_z \tag{A.4}$$

Equation (A. 1) and (A. 4) may now be specialized for the case of equation (10) of the text, using (A. 3). Equation (A. 1) may be evaluated exactly as:

$$N = \frac{n_m\,\Delta^{1/2}}{2\pi^2\,\alpha^{1/2}\,(\beta^2/2\Delta)}\int_0^\infty\left[\left(\frac{E}{\Delta}\right)^{1/2}+\frac{2}{3}\left(\frac{E}{\Delta}\right)^{3/2}\right] f_0\left(\frac{E-E_F}{kT}\right)dE \tag{A.5}$$

where n_m is the number of minima in the conduction band. This may be written in the form

$$F_{1/2}(\eta)\left[1+\frac{2}{3}\,\frac{kT}{\Delta}\,\frac{F_{3/2}(\eta)}{F_{1/2}(\eta)}\right] = \frac{\sqrt{\pi}}{2}\,\frac{N}{N_c} \tag{A.6}$$

Here
$$N_c = \frac{n_m}{\sqrt{2}}\left(\frac{kT}{2\pi}\right)^{3/2}\frac{1}{\alpha^{1/2}\,(\beta^2/2\Delta)} = 2\,n_m\left(\frac{2\pi\,m^{**}kT}{h^2}\right)^{3/2} \tag{A.7}$$

where m^{**} is the density of states effective mass, and

$$F_p(\eta) = \int_0^\infty \frac{x^p}{1+e^{x-\eta}}\,dx \tag{A.8}$$

the Fermi-Dirac integral tabulated by BEER, CHASE and CHOQUARD[21] with $\eta = E_F/kT$.

Equation (A. 4) can also be evaluated exactly; the k_z integration takes the form:

$$\int_{-(E/\alpha)^{1/2}}^{+(E/\alpha)^{1/2}} -\frac{E+\Delta-\alpha k_z^2}{2\pi^2\hbar^2}\left[\frac{1}{3}-\frac{1}{3}\,\frac{\Delta^2}{(E+\Delta-\alpha k_z^2)^2}+\frac{4}{3}\,\frac{\alpha^2k_z^2}{\beta^2}\right]dk_z \tag{A.9}$$

In practice we are only interested in values of E such that $E-\alpha k_z^2 \ll \Delta$. Hence, it is most convenient to expand the integrand in terms of $(E-\alpha k_z^2)\Delta$ retaining only the two lowest orders. Equations (A. 9) then reduces to:

$$\left.\begin{aligned}\int_{-(E/\alpha)^{1/2}}^{(E/\alpha)^{1/2}} dk_z &= \frac{\Delta}{2\pi^2\hbar^2}\,\frac{2}{3}\int_{-(E/\alpha)^{1/2}}^{(E/\alpha)^{1/2}} dk_z\left[\frac{E-\alpha k_z^2}{\Delta}\left\{1-\frac{1}{2}\,\frac{E-\alpha k_z^2}{\Delta}+\right.\right.\\ &\left.\left.+\frac{2\,\alpha^2k_z^2}{\beta^2}\right\}+\frac{2\Delta}{3\pi^2\hbar^2}\,\frac{\alpha^2k_z^2}{\beta^2}\right] =\\ &= \frac{2}{3\pi^2\hbar^2}\,\frac{E^{3/2}}{\alpha^{1/2}\,(\beta^2/2\Delta)}\left(\frac{1}{3}\,\alpha+\frac{2}{3}\,\frac{\beta^2}{2\Delta}\right)\cdot\left\{1-\frac{2}{5}\,\frac{E}{\Delta}\,\frac{1-\alpha\Delta/\beta^2}{1+\alpha\Delta/\beta^2}\right\}\end{aligned}\right\} \tag{A.10}$$

If we carry out the E integration we find:

$$\frac{N}{m^*} = \frac{1}{\hbar^2}\left(\frac{2}{3}\,\alpha + \frac{2}{3}\,\frac{\beta^2}{\Delta}\right)\frac{2}{\sqrt{\pi}}\,N_c\left[F_{1/2}(\eta) - \frac{2}{3}\,\frac{kT}{\Delta}\,\frac{1-\alpha\Delta/\beta^2}{1+\alpha\Delta/\beta^2}\,F_{3/2}(\eta)\right] \tag{A.11}$$

Combining (A. 11) with (A. 7) to eliminate N_c we obtain finally

$$\frac{1}{m^*} = \frac{1}{3}\left(\frac{1}{m_{\|}} + \frac{2}{m_{\perp}}\right)\left[1 - \frac{2}{3}\,\frac{kT}{\Delta}\,\frac{2}{1+m_{\perp}/2\,m_{\|}}\,\frac{F_{3/2}(\eta)}{F_{1/2}(\eta)}\right] \tag{A.12}$$

correct to order kT/Δ, where

$$\frac{1}{m_{\|}} = \frac{2\,\alpha}{\hbar^2}, \quad \frac{1}{m_{\perp}} = \frac{\beta^2}{\hbar^2\Delta} \tag{A.13}$$

$$m^{**} = (m_{\|}\,m_{\perp}^{\,2})^{1/3}$$

References

1) Spitzer, W. G., and Fan, H. Y., Phys. Rev. *106*, 882 (1957).
2) Cardona, M., Paul, W., and Brooks, H. J., Phys. Chem. of Solids *8*, 204 (1959).
3) Herring, C., and Vogt, E., Phys. Rev. *101*, 944 (1956).
4) Brooks, H., Advances in Electronics and Electron Physics, 7, 85.
5) Ham, F., Phys. Rev. *100*, 1251*A* (1955).
6) Goldberg, C., Phys. Rev. *109*, 337 (1958); glicksman, M., Phys. Rev. *108*, 264 (1957).
7) Keesom, P., Seidel, G., Phys. Rev. *113*, 33 (1959).
8) Bowers, R., J. Phys. Chem. of Solids *8*, 210 (1959).
9) Stevens, P. K., Leland, J. W., Crawford, J. H., and Schweinler, H. C., Phys. Rev. *100*, 1084 (1955).
10) Geist, D., Die Naturwissenschaften *45*, 33 (1958).
11) McFarlane, G. G., McLean, T. P., Quarrington, J. E., and Roberts, V., Phys. Rev. *108*, 1377 (1957).
12) Sonder, E., and Stevens, D. K., Phys. Rev. *110*, 1027 (1958).
13) McFarlane, G. G. McLean, T. P., Quarrington, J. E., and Roberts, V., Phys. Rev. *111*, 1245 (1958).
14) Kaiser, W., Collins, R. J., and Fan, H. Y., Phys. Rev. *91*, 1380 (1953).
15) Nathan, J. I., Paul, W. and Brooks, H., Am. Phys. Soc. Bull. *3*, 14 (1958).
16) Seitz, F., Modern Theory of Solids (McGraw-Hill, New York).
17) Trumbore, F. A., and Tartaglia, A. A., J. App. Phys. *29*, 1511 (1958).
18) Phillips, J. C., Private Communication.
19) Philipp, H. R., and Taft, E. A., Phys. Rev. *113*, 1002 (1959).
20) Roth, L. M., and Lax, B., Phys. Rev. Letters *3*, 217 (1959).
21) Beer, A. C., Chase, M. N., and Choquard, P. F., Helv. Phys. Acta *28*, 529 (1955).
22) Kane, E. O., J. Phys. Chem. of Solids *1*, 82 (1956).